Journal de Mécanique,
Vol. 19, N° 1, 1980

Normal-mode analysis for the oscillations of a viscous liquid drop in an immiscible liquid

by

Andrea PROSPERETTI*

ABSTRACT. — An analytical and numerical study of the normal modes for the small-amplitude oscillations of a viscous liquid drop in an immiscible viscous liquid is given. The limiting cases of a viscous drop in vacuum and of a bubble of fixed volume are also considered. The presence of a continuous spectrum, not noticed by previous investigators, is recognized. A comparison of the theory with some experimental data is presented. It is concluded that there is a satisfactory agreement between theoretical and measured oscillations frequencies. Agreement for the damping constants, although much improved over that previously reported by other authors, is however still not satisfactory.

RÉSUMÉ. — On étudie analytiquement et numériquement les modes normaux d'oscillation de petite amplitude d'une goutte de liquide visqueux dans un liquide visqueux non miscible. On considère aussi les situations limites d'une goutte visqueuse dans le vide et d'une bulle dans un liquide visqueux. On montre la présence d'un spectre continu, qui n'a pas été mis en évidence par les chercheurs précédents. On présente une comparaison de la théorie avec des résultats expérimentaux, qui montre un accord satisfaisant pour les fréquences d'oscillation. Cependant, une différence importante subsiste entre la théorie et l'expérience pour les constants d'amortissement. De toute façon cette différence est très réduite par rapport aux résultats déjà publiés.

* Istituto di Fisica, Università di Milano, 20133 Milano, Italy.

JOURNAL DE MÉCANIQUE. — 0021-7832/1980/149/$ 5.00/

1. Introduction

We present in this paper a detailed analytical and numerical study of the spectrum of the boundary-value problem posed by small-amplitude (linear) oscillations of viscous liquid drops about the spherical shape. We consider the case of a drop immersed in an immiscible viscous liquid, as well as the two limiting situations of a drop in vacuum and of a gas or vapor bubble of fixed volume. Aside from the limitations inherent in the linearization of the problem, other approximations made here include the neglect of external forces (notably gravity and the related buoyancy effects), of effects due to boundaries, of the interaction with other droplets or bubbles, and, perhaps more importantly, of the relative motion between the bubble or droplet and the host liquid. Information about the last two points can be found in references [1]-[3]. In general one can say however that the validity of our approximations increases as the radius of the droplet gets smaller. As will be seen below, in this region of small radii viscous effects are particularly important and it is precisely interest in these effects that has originated the present investigation.

The study of the spectrum implies the separation of the time variable and the analysis of the pseudo steady-states of the system. Thus, in the present study, we do not give any information on the related initial-value problem. Although our results are in principle sufficient to solve this problem it is well-known that this is not so in practice because of the complexity of the operations required. The initial-value problem is studied by means of an alternative, more efficient, method specifically designed for this purpose in [4] and [31].

The system considered here models a physical situation which is encountered quite frequently in experimental research and industrial practice. The occurrence of flows which include bubbles or droplets of an immiscible liquid is quite widespread in the chemical industry, where this configuration provides a large interfacial area, in heat transfer apparatuses, in combustion, in the oil industry, in atmospheric sciences, and in some biological contexts. A somewhat unconventional application occurs in nuclear physics in the liquid-drop model of the atomic nucleus. A survey of these applicative aspects of our subject and extensive bibliographies can be found in the various papers collected in [5]. Recently it has also been shown that single droplets suspended in a host liquid can be used for studies of tensile strengths ([27], [28]), of the mechanical properties of interfaces [29] and of biological materials, and emulsification [30].

After the early studies of Lord Kelvin [6] and Lord Rayleigh [7] for the inviscid case and of Lamb [8] for small viscosity, the first analyses of the present problem valid for any viscosity were given by Chandrasekhar ([9], [10]) and Reid [11]. All these authors considered however only the limiting cases of gas or vapor bubbles, or of droplets in vacuum. The first paper devoted to the two-fluid case is that of Valentine *et al* [12] who did not properly account for the effects of the viscous boundary layer adjacent to the droplet. This error was later noticed and corrected by Miller and Scriven [13], who included in their analysis also the rheological properties of the interface. They failed to realize, however, the presence of the continuous spectrum. Furthermore, they did not give a numerical illustration of their results the analytical form of which, by the very nature of the problem, is not very suggestive. More recent contributions are those of Tong and Wong [14], who gave a numerical study of the drop-in-vacuum case, including the effect of surface and volume charges, and who attempted to obtain estimates of the nuclear viscosity [15].

In concluding these introductory remarks it is appropriate to consider briefly the limits of validity of our approximations. Clearly, the neglect of interactions with other droplets will be justified whenever the mean separation of the droplets is large compared with the mean radius. Similarly, when the boundaries are at a distance from the droplet which is large compared with the radius, their effect will also be negligible. For what concerns the relative motion between the droplet and the host liquid we may say that it will be unimportant provided that $U/\omega \ll R$, where ω is the frequency of oscillation, U the velocity of the relative motion, and R the mean radius of the droplet. For instance, for rise under the action of buoyancy forces, we may estimate U by the Hadamard-Rybczynski formula (*see* e. g. reference [8], p. 600):

$$U = \frac{2R^2 g(\rho_0 - \rho_i)(\mu_0 + \mu_i)}{3\mu_0(2\mu_0 + 3\mu_i)},$$

where g is the acceleration of gravity and $\rho_0 \mu_0$, $\rho_i \mu_i$ are the density and viscosity of the host and droplet fluid. Estimating the order of magnitude of ω by the result for the inviscid frequency of the lowest mode [i. e. equation (34) below for $n=2$] the inequality $U/\omega \ll R$ gives:

$$R \ll \left\{ \frac{54\zeta}{2\rho_0 + 3\rho_i} \left[\frac{\mu_0(2\mu_0 + 3\mu_i)}{g(\rho_0 - \rho_i)(\mu_0 + \mu_i)} \right]^2 \right\}^{1/5},$$

where ζ denotes the surface tension coefficient.

2. Mathematical formulation

We adopt a spherical polar coordinate system (r, θ, φ) centered at the centroid of the drop and we describe the free surface by:

$$F(r, \theta, \varphi; t) \equiv r - R - a(t) Y_n^m(\theta, \varphi) = 0, \tag{1}$$

where R is the (fixed) radius of the unperturbed spherical drop, a is the amplitude of the n-th order mode, and Y_n^m is a spherical harmonic. In the linearized approximation the different modes are uncoupled so that we can consider each one of them separately from the others. It will be seen that only the index n will enter in the following developments.

We assume that both the inner and outer fluid are incompressible, so that:

$$\nabla . \mathbf{u} = 0, \tag{2}$$

and that their motion satisfies the linearized Navier-Stokes equations:

$$\rho \frac{\partial \mathbf{u}}{\partial t} = -\nabla p - \mu \nabla \times \nabla \times \mathbf{u}. \tag{3}$$

In equations (2) and (3) $\mathbf{u}$ and p denote the velocity and pressure fields, t is the time, ρ is the density, and μ is the viscosity. In the following the subscripts i and o will be attached to quantities pertaining to the inner and outer fluid respectively. The absence of a subscript indicates that a statement is applicable to both fluids. Taking the curl of equation (3) we obtain the following equation for the vorticity $\boldsymbol{\omega} = \nabla \times \mathbf{u}$:

$$\frac{\partial \boldsymbol{\omega}}{\partial t} = -\nu \nabla \times \nabla \times \boldsymbol{\omega}, \tag{4}$$

where $\nu = \mu/\rho$ is the kinematic viscosity.

On the boundary $F = 0$ we shall impose that the discontinuity in normal stresses be balanced by surface tension, and that the tangential stresses and tangential velocities be continuous. In addition we shall apply there the usual kinematic boundary condition in the form:

$$\frac{\partial F}{\partial t} + \mathbf{u} . \nabla F = 0. \tag{5}$$

Boundedness of velocity and pressure at the origin and at infinity will also be required.

For the study of the eigenvalue spectrum we assume for every quantity a time dependence proportional to $\exp(-\sigma t)$, where σ, the eigenvalues, are complex constants. Accordingly, we can make the following substitution wherever the operator of time differentiation appears:

$$\frac{\partial}{\partial t} \to -\sigma. \tag{6}$$

It can readily be shown that, if σ is an eigenvalue, its complex conjugate $\bar{\sigma}$ is also one. Hence we shall write:

$$\sigma = b + i\omega, \tag{7}$$

and we shall take ω to be positive or zero. On physical grounds it is also obvious that $b \geqq 0$.

By definition, the vorticity field $\boldsymbol{\omega}$ is solenoidal and therefore it admits a vector potential which we shall decompose into two parts writing:

$$\boldsymbol{\omega} = \nabla \times (\mathbf{A} + \nabla \times \mathbf{B}). \tag{8}$$

The auxiliary fields $\mathbf{A}$ and $\mathbf{B}$ can be taken to have the form:

$$\begin{cases} \mathbf{A} = \mathrm{T}(r)\, \mathrm{Y}_n^m(\theta.\ \varphi) e^{-\sigma t} \hat{\mathbf{r}}, \\ \mathbf{B} = \mathrm{S}(r)\, \mathrm{Y}_n^m(\theta.\ \varphi) e^{-\sigma t} \hat{\mathbf{r}}, \end{cases} \tag{9}$$

where $\hat{\mathbf{r}}$ is the unit vector in the radial direction. The decomposition (8), with $\mathbf{A}$ and $\mathbf{B}$ given by (9), corresponds to the decomposition into toroidal and poloidal components described in [10], Appendix 3, and in [16]. Substitution of (8) into (4) gives, after some straightforward manipulations, the following identical equations for the poloidal and toroidal amplitudes $\mathrm{S}(r)$ and $\mathrm{T}(r)$:

$$\nu \frac{d^2 \mathrm{S}}{dr^2} + \sigma \mathrm{S} - \nu \frac{n(n+1)}{r^2} \mathrm{S} = 0, \tag{10}$$

$$\nu \frac{d^2 \mathrm{T}}{dr^2} + \sigma \mathrm{T} - \nu \frac{n(n+1)}{r^2} \mathrm{T} = 0. \tag{11}$$

Here use has been made of (6) to eliminate the time derivative.

From equation (8) the velocity field $\mathbf{u}$ can be obtained as:

$$\mathbf{u} = \mathbf{A} + \nabla \times \mathbf{B} + \nabla \varphi. \tag{12}$$

The scalar φ must be such that the incompressibility condition (2) is satisfied, which leads to:

$$\nabla^2 \varphi = -\mathbf{V}.\mathbf{A} = -\frac{1}{r^2}\frac{\partial}{\partial r}(r^2 \mathrm{T}) \mathrm{Y}_n^m e^{-\sigma t}.$$

Putting:

$$\varphi = \Phi(r) \mathrm{Y}_n^m(\theta, \varphi) e^{-\sigma t},$$

the general solution of this equation can readily be obtained as:

$$\Phi = \left[\alpha - \frac{n+1}{2n+1}\int_{\mathrm{R}}^{r} s^{-n}\mathrm{T}(s)\,ds\right] r^n + \left[\beta - \frac{n}{2n+1}\int_{\mathrm{R}}^{r} s^{n+1}\mathrm{T}(s)\,ds\right] r^{-(n+1)}, \tag{13}$$

where α and β are integration constants. Boundedness for $r=0$ requires that:

$$\beta_i = -\frac{n}{2n+1}\int_0^{\mathrm{R}} r^{n+1}\mathrm{T}(r)\,dr, \tag{14}$$

whereas boundedness for $r \to \infty$ is insured if:

$$\alpha_0 = \frac{n+1}{2n+1}\int_{\mathrm{R}}^{\infty} r^{-n}\mathrm{T}(r)\,dr. \tag{15}$$

Finally equation (3) allows to express the pressure fields in terms of the other quantities. One readily finds the following expressions:

$$\begin{cases} p_i = \mathrm{P}_i + \rho_i\left(\sigma\varphi_i - \nu\dfrac{\partial \mathrm{T}_i}{\partial r}\mathrm{Y}_n^m\right), \\ p_0 = \mathrm{P}_\infty + \rho_0\left(\sigma\varphi_0 - \nu\dfrac{\partial \mathrm{T}_0}{\partial r}\mathrm{Y}_n^m\right). \end{cases} \tag{16}$$

The constant P_∞ has the physical meaning of the ambient pressure, i. e. the pressure at a distance from the drop. The other integration constant P_i is related to it by Laplace's formula, which expresses the condition of equilibrium for the unperturbed spherical drop [17],

$$\mathrm{P}_i - \mathrm{P}_\infty = \frac{2\zeta}{\mathrm{R}},$$

where ζ is the surface tension constant.

To the order of approximation retained here the condition of continuity of the tangential velocity requires that:

$$\Phi_i(R)=\Phi_0(R), \tag{17}$$

$$S_i(R)=S_0(R), \tag{18}$$

and the linearized form of the kinematical boundary condition (5) requires that:

$$T(R)+\left.\frac{\partial\Phi}{\partial r}\right|_{r=R}=-\sigma a, \tag{19}$$

where $a(t)=ae^{-\sigma t}$. Continuity of the tangential stresses is expressed by:

$$\frac{d}{dr}[r^{-2}(\mu_0 S_0-\mu_i S_i)]_{r=R}=0, \tag{20}$$

$$2R\frac{d}{dr}[r^{-1}(\mu_0\Phi_0-\mu_i\Phi_i)]_{r=R}+\mu_0 T_0(R)-\mu_i T_i(R)=0. \tag{21}$$

Inserting the expression (13) for Φ into the kinematical boundary conditions (19) it is readily established that:

$$\begin{cases} \beta_0=\dfrac{n}{n+1}R^{2n+1}\alpha_0+\dfrac{\sigma}{n+1}R^{n+2}a, \\ \alpha_i=\dfrac{n+1}{n}R^{-(2n+1)}\beta_i-\dfrac{\sigma}{n}R^{-(n-1)}a. \end{cases} \tag{22}$$

With these results the condition (17) of equality of tangential velocities reduces to:

$$nR^{n-1}\alpha_0-(n+1)R^{-(n+2)}\beta_i=-\sigma a, \tag{23}$$

while the condition (21) of equality of tangential stresses gives:

$$\begin{aligned} 2n(2n+1)\mu_0 R^{n-1}\alpha_0-2(n+1)(2n+1)\mu_i R^{-(n+2)}\beta_i \\ +n(n+1)[\mu_0 T_0(R)-\mu_i T_i(R)] \\ =-2[n(n+2)\mu_0-(n-1)(n+1)\mu_i]\sigma a. \end{aligned} \tag{24}$$

The following two expressions for the pressure at the interface will also be useful:

$$\begin{cases} p_0(R)=P_\infty+[n\mu_0 T_0(R)/R+\rho_0 R\sigma^2 a/(n+1)]Y_n^m, \\ p_i(R)=P_i-[(n+1)\mu_i T_i(R)/R+\rho_i R\sigma^2 a/n]Y_n^m. \end{cases} \tag{25}$$

These results can be obtained from (16) making use of (13), (22), (11) and integration by parts.

The last boundary condition requires that surface tension balance the discontinuity in the normal stresses. Making use of (25) one readily finds:

$$(26)\quad \left[\left(\frac{\rho_0}{n+1}+\frac{\rho_i}{n}\right)\sigma^2 R+2(n-1)(n+2)(\mu_0-\mu_i)\frac{\sigma}{R} +(n+2)(n-1)\frac{\zeta}{R^2}\right]a +n(n+2)\mu_0\frac{T_0(R)}{R}-(n-1)(n+1)\mu_i\frac{T_i(R)}{R}=0.$$

If now $T_0(R)$ and $T_i(R)$ can be expressed as (linear) functions of a, this equation reduces to the characteristic equation for σ. To this end it is necessary to solve equation (11) subject to the conditions (23) and (24). This problem will be treated in the following section.

An analysis of the previous results shows that the problems for the poloidal and toroidal components are effectively uncoupled. Hence we find two families of normal modes, those for which S vanishes while a and T are different from zero, and those for which $a=0$, $T=0$, and $S\neq 0$. It is obvious that only the first set of modes is associated with shape oscillations of the drop. The second family of modes describes a motion in which the different fluid shells rotate about their centers, and have been called in [13] "shear waves" or "purely rotational waves". Since there is no restoring force for this kind of motion, it is natural to expect that these modes will be aperiodically damped. We shall analyze them briefly in Section 8.

Finally, notice that, since S and T are eigenfunctions of a linear problem, they are only determined up to an arbitrary constant multiplicative factor which can be fixed, for instance, by a suitable normalization.

3. The discrete spectrum

The following change of dependent variable:

$$U(r)=r^{-1/2}T(r),$$

puts equation (11) into the standard form of Bessel's equation:

$$\frac{d^2U}{dr^2}+\frac{1}{r}\frac{dU}{dr}+\left[\frac{\sigma}{\nu}-\frac{(n+(1/2))^2}{r^2}\right]U=0,$$

the general solution of which may be written either as:

$$T(r)=x^{1/2}[KH^{(1)}_{n+(1/2)}(x)+LH^{(2)}_{n+(1/2)}(x)]. \tag{27 a}$$

or as:

$$T(r)=x^{1/2}[MJ_{n+(1/2)}(x)+NY_{n+(1/2)}(x)]. \tag{27 b}$$

In these equations:

$$x=r\left(\frac{\sigma}{\nu}\right)^{1/2}.$$

In order to make the square root unique we shall cut the complex plane along the negative real axis. Since we have already assumed that $\omega=\text{Im }\sigma\geqq 0$, this choice has the consequence that Im $x\geqq 0$.

We consider in this section the case in which Im σ is strictly positive. On the basis of the known asymptotic behavior of Bessel's functions we find then that boundedness at $r=0$ requires to take:

$$T_i(r)=\left(\frac{r}{R}\right)^{1/2}T_i(R)\frac{J_{n+(1/2)}(x_i)}{J_{n+(1/2)}(X_i)}, \tag{28}$$

whereas boundedness at infinity requires that the solution in the outer fluid be chosen in the form (27 *a*) with $L_0=0$,

$$T_0(r)=\left(\frac{r}{R}\right)^{1/2}T_0(R)\frac{H^{(1)}_{n+(1/2)}(x_0)}{H^{(1)}_{n+(1/2)}(X_0)}. \tag{29}$$

In these equations the unknown surface values have been inserted explicitly and:

$$X=R\left(\frac{\sigma}{\nu}\right)^{1/2}.$$

Substitution of (28) into (14) results in:

$$R^{-(n+2)}\beta_i=-\frac{n}{2n+1}\frac{T_i(R)}{\mathcal{J}_{n+(3/2)}(X_i)}, \tag{30}$$

where:

$$\mathcal{J}_\nu(z)=zJ_{\nu-1}(z)/J_\nu(z),$$

is the quotient of Bessel's functions of the first kind defined and studied in [18]. Similarly, substituting (29) into (15) one finds:

$$R^{n-1}\alpha_0=\frac{n+1}{2n+1}\frac{T_0(R)}{\mathcal{H}^{(1)}_{n-(1/2)}(X_0)}, \tag{31}$$

where:

$$\mathscr{H}_{\nu}^{(1)}(z)=z\,\mathrm{H}_{\nu+1}^{(1)}(z)/\mathrm{H}_{\nu}^{(1)}(z),$$

is a quotient of Hankel's functions [18].

Substitution of (30) and (31) into (23), (24) and solution of the resulting system for $\mathrm{T}_0(\mathrm{R})$, $\mathrm{T}_i(\mathrm{R})$ yields:

$$(32)\quad \begin{cases} \mathrm{T}_i(\mathrm{R})= \dfrac{(2n+1)\mu_0\,\mathscr{H}_{n-(1/2)}^{(1)}(\mathrm{X}_0)-2(n-1)(n+1)(\mu_0-\mu_i)}{\left\{\begin{array}{l} n(n+1)[2(\mu_i-\mu_0) \\ \qquad -\mu_i\mathscr{J}_{n+(3/2)}(\mathrm{X}_i)-\mu_0\,\mathscr{H}_{n-(1/2)}^{(1)}(\mathrm{X}_0)] \end{array}\right\}} \\ \qquad\qquad \times\mathscr{J}_{n+(3/2)}(\mathrm{X}_i)\,\sigma a, \\ \mathrm{T}_0(\mathrm{R})= \dfrac{(2n+1)\mu_i\mathscr{J}_{n+(3/2)}(\mathrm{X}_i)-2n(n+2)(\mu_i-\mu_0)}{\left\{\begin{array}{l} n(n+1)[2(\mu_i-\mu_0) \\ \quad -\mu_i\mathscr{J}_{n+(3/2)}(\mathrm{X}_i)-\mu_0\,\mathscr{H}_{n-(1/2)}^{(1)}(\mathrm{X}_0)] \end{array}\right\}} \\ \qquad\qquad \times\mathscr{H}_{n-(1/2)}^{(1)}(\mathrm{X}_0)\,\sigma a. \end{cases}$$

We can now insert these expressions into (26) to obtain the following characteristic equation for the discrete spectrum:

$$\begin{aligned}(33)\quad & \mathrm{R}^2[n\rho_0+(n+1)\rho_i][\mu_i\mathscr{J}_{n+(3/2)}(\mathrm{X}_i) \\ & \quad +\mu_0\,\mathscr{H}_{n-(1/2)}^{(1)}(\mathrm{X}_0)+2(\mu_0-\mu_i)]\times(\sigma^2+\omega^2) \\ & -\sigma[(2n+1)\mu_i\mathscr{J}_{n+(3/2)}(\mathrm{X}_i)+2n(n+2)(\mu_0-\mu_i)] \\ & \quad \times[(2n+1)\mu_0\,\mathscr{H}_{n-(1/2)}^{(1)}(\mathrm{X}_0)-2(n-1)(n+1)(\mu_0-\mu_i)]=0,\end{aligned}$$

where:

$$(34)\qquad \omega^2=\frac{(n-1)n(n+1)(n+2)}{n\rho_0+(n+1)\rho_i}\,\frac{\zeta}{\mathrm{R}^3},$$

is the frequency of oscillation of the inviscid problem ([8], p. 475). After some simplifications the characteristic equation given by Miller and Scriven [13] can be reduced to this form.

4. The continuous spectrum

Let us consider now whether purely real values of σ exist, i.e. eigenvalues such that $\omega=\mathrm{Im}\ \sigma=0$. If we choose to write the solution to (11) in the form (27 *b*), again boundedness for $r\to 0$ requires that $\mathrm{N}_i=0$ so that for the inner fluid we still find the previous result (28). The situation is however different

for the outer fluid, since both $J_{n+(1/2)}(x)$ and $Y_{n+(1/2)}(x)$ tend to zero for $x \to \infty$ on the real line. Hence we write the solution in the outer fluid in the form (27 *b*). Notice however that, for $r \to \infty$, $T_0(r)$ as given by (27 *b*) is asymptotic to [19] :

$$(35)\quad T_0(r) \sim \left(\frac{2}{\pi}\right)^{1/2} \left\{ M_0 \cos\left[x_0 - (n+1)\frac{\pi}{2}\right] + N_0 \sin\left[x_0 - (n+1)\frac{\pi}{2}\right]\right\}.$$

The failure of this expression to become small at large distances conforms with the general behavior of the eigenfunctions of the continuous spectrum in an unbounded domain [20]; we shall return on the physical meaning of this feature at the end of this section.

Substitution of (27 *b*) into (15) results in:

$$R^{n-1}\alpha_0 = \frac{n+1}{2n+1} X_0^{-1/2}[M_0 J_{n-(1/2)}(X_0) + N_0 Y_{n-(1/2)}(X_0)].$$

With this expression for α_0 and the one for β_i given in equation (30) we can put equations (23) and (24) into the following form:

$$(36\,a)\quad X_0^{-1/2} J_{n-(1/2)}(X_0) M_0 + X_0^{-1/2} Y_{n-(1/2)}(X_0) N_0 + [\mathscr{J}_{n+(3/2)}(X_i)]^{-1} T_i(R) = -\frac{2n+1}{n(n+1)}\sigma a,$$

$$(36\,b)\quad [2X_0^{-1/2} J_{n-(1/2)}(X_0) + X_0^{1/2} J_{n+(1/2)}(X_0)]\,\mu_0 M_0 + [2X_0^{-1/2} Y_{n-(1/2)}(X_0) + X_0^{1/2} Y_{n+(1/2)}(X_0)]\,\mu_0 N_0 + \{2[\mathscr{J}_{n+(3/2)}(X_i)]^{-1} - 1\}\,\mu_i T_i(R) = 2\left(\frac{n-1}{n}\mu_i - \frac{n+2}{n+1}\mu_0\right)\sigma a,$$

whereas the condition on the normal stresses, equation (26), becomes:

$$(37)\quad n(n+2)\mu_0 J_{n+(1/2)}(X_0) M_0 + n(n+2)\mu_0 Y_{n+(1/2)}(X_0) N_0 - (n-1)(n+1)\mu_i T_i(R) = -\left[\left(\frac{\rho_0}{n+1} + \frac{\rho_i}{n}\right)\sigma^2 R^2 + 2(n-1)(n+2)(\mu_0 - \mu_i)\sigma + \frac{\zeta}{R}(n-1)(n+2)\right] a.$$

These three equations, viewed as a linear system in the three unknowns M_0, N_0, $T_i(R)$, may be solved to yield expressions for these quantities in terms of the amplitude a of the surface distorsion for any (real, non-negative) value of σ. In addition to the discrete point spectrum found in the previous section we thus find a continuous spectrum consisting of the entire positive real semi-axis of the σ-plane. As already remarked this result is not unexpected in view of the unboundedness of the domain (*see* e. g. [8], p. 628, for the analogous plane problem). Furthermore, as will be shown below, the eigenfunctions would not form a complete system without the inclusion of the continuous spectrum. The importance of this part of the spectrum is apparent in the initial-value approach to this problem, where it appears as a cut in the complex plane of the Laplace-transformed variable conjugate to the time t.

It may appear that the failure of the eigenfunctions to approach zero as $r \to \infty$ exhibited in (35) offers some difficulty of interpretation of the physical meaning of the continuous spectrum. This feature is quite familiar in other fields where normal-mode approaches are normally used, such as quantum mechanics ([21], [22]), and also in fluid mechanics ([8], p. 628; [23]), where however it is less commonly encountered in the explicit form found here. The problem may be resolved by realizing that, even in principle, the motion corresponding to a single eigenvalue of the continuous spectrum cannot be realized in a real physical situation because it would involve an infinite amount of energy at the initial instant. However, *superpositions* of eigenfunctions of the continuous spectrum can be realized which give rise to a finite energy and describe for $t=0$ a distribution of vorticity in some finite region of the outer fluid. For $t>0$ this distribution of vorticity spreads outwards (and inwards) while its maximum value decreases exponentially with time. Thus the significance of the normal modes of the continuous spectrum can only be understood in the context of an initial-value approach to the problem [4]. Their inclusion among the eigenfunctions is essential to describe the (damped) propagation of vorticity "wave-packets" to infinity. Another fluid dynamic problem where a continuous spectrum is present alongside a discrete one has recently been studied in [32].

5. Viscous liquid drop in vacuum

Let us consider first the limiting situation in which the outer fluid has vanishing dynamical effects as would happen, for instance, for a drop in vacuum or in air. The appropriate form of the preceding general results can

be obtained by letting $\mu_0 \to 0$, $\rho_0 \to 0$ in all the equations. Taking this limit and noticing that:

$$\mathscr{H}^{(1)}_{n-(1/2)}(X) \simeq -iX + n + \frac{1}{2} in(n-1)X^{-1}, \quad \text{for} \quad X \to \infty, \tag{38}$$

we find:

$$T_i(R) = \frac{\mathscr{J}_{n+(3/2)}(X_i)}{1-(1/2)\mathscr{J}_{n+(3/2)}(X_i)} \frac{n-1}{n} \sigma a,$$

$$(\sigma^2 + \omega_D^2 - 2b_D\sigma)[\mathscr{J}_{n+(3/2)}(X_i) - 2] + 4(n-1)^2(n+1)(\nu_i/R^2)\sigma = 0, \tag{39}$$

where:

$$\begin{cases} \omega_D^2 = (n-1)n(n+2)\zeta/(\rho_i R^3), \\ b_D = (n-1)(2n+1)\nu_i/R^2. \end{cases} \tag{40}$$

It may readily be established that ω_D is the frequency of oscillation of a drop of an inviscid liquid and that b_D is the damping constant for small viscosity ([8], p. 475 and p. 639). Indeed, since:

$$\begin{aligned} \mathscr{J}_{n+(1/2)}(X) \simeq{}& X\cot\left(X - \frac{n}{2}\pi\right) \\ & - \frac{1}{2}n\left[n - 1 + (n+1)\cot^2\left(X - \frac{n}{2}\pi\right)\right] \\ & + \frac{1}{X}\cot\left(X - \frac{n}{2}\pi\right)\frac{n(n+1)}{4} \\ & \times\left[(n-1)(n+2) + n(n+1)\cot^2\left(X - \frac{n}{2}\pi\right)\right], \quad \text{for} \quad X \to \infty, \end{aligned} \tag{41}$$

we obtain from (39) the following approximate form of the characteristic equation, valid for small viscosity:

$$\sigma^2 - 2b_D\sigma + \omega_D^2 \simeq 0, \tag{42}$$

which proves the previous assertion. The opposite limiting case of large viscosity can be investigated with the aid of the result [18]:

$$\mathscr{J}_{n+(1/2)}(X) \simeq 2n + 1 - \frac{1}{2n+3}X^2, \quad \text{for} \quad X \to 0. \tag{43}$$

The least damped normal mode is thus found to be:

$$\sigma \simeq \frac{2n+1}{2(n-1)(2n^2+4n+3)} \frac{R^2\omega_D^2}{\nu_i}.$$

The characteristic equation (39) was first given by Chandrasekhar for the case of a gravitating liquid spheroid ([9], [10]), and shown by Reid [11] to apply also to the liquid drop case provided that ω_D^2 is defined as in (40). It is readily shown that for each n it has an infinity of solutions with positive real parts ([9], [10]). Furthermore, since $\overline{\mathscr{J}_{n+(3/2)}(X_i)}=\mathscr{J}_{n+(3/2)}(\overline{X}_i)$ (where the bar denotes the complex conjugate) it is clear that the complex solutions occur in pairs.

We shall limit our considerations here to the root of (39) possessing the smallest real part, which corresponds to the least damped normal mode. If the following non-dimensional quantities are introduced:

$$\sigma_*=(\rho_i R^3/\zeta)^{1/2}\sigma, \qquad \varepsilon_i=\nu_i(\rho_i/R\zeta)^{1/2}, \tag{44}$$

it can be seen from (39) that, for fixed n, the nondimensional eigenvalue σ_* is a function of the single parameter ε_i, which may be regarded as a nondimensional viscosity. The real part of this function,

$$b_*=\mathrm{Re}\,\sigma_*,$$

which represents the damping constant for small-amplitude oscillations, is plotted as a function of ε_i in Figure 1 for $n=2$, 3, and in Figure 2 for $n=4$, 5, 6. In Figure 1 also the real part of the nondimensional solution of (42) is shown as a dashed line. It is seen that the exact and approximate results agree for small ε, but that for larger values of viscosity the result predicted by (42) lies consistently above the correct one. This circumstance is also encountered in the plane case [24] and in the bubble case to be examined in the next Section.

Figures 3 and 4 show $\omega_*=\mathrm{Im}\,\sigma_*$ as determined from (39) and (42). Again the two results agree for small ε_i. It is seen that ω_* vanishes for ε_i greater than a critical value. This behavior corresponds to the fact that for sufficiently large viscosity the motion of the drop turns from damped oscillations to an aperiodic relaxation towards equilibrium. In Figures 1 and 2 it is observed that in correspondence with the critical value of ε_i, b_* bifurcates into a pair of curves one of which grows very rapidly whereas the other one tends to zero for large ε_i exhibiting the characteristics of the "creeping" motion of a strongly overdamped oscillator [10].

6. Gas bubble

We now turn to the other limiting case in which it is the inner fluid to have negligible dynamical effects. This would be the situation, for instance, for the oscillations about the spherical shape of a stable gas or vapor

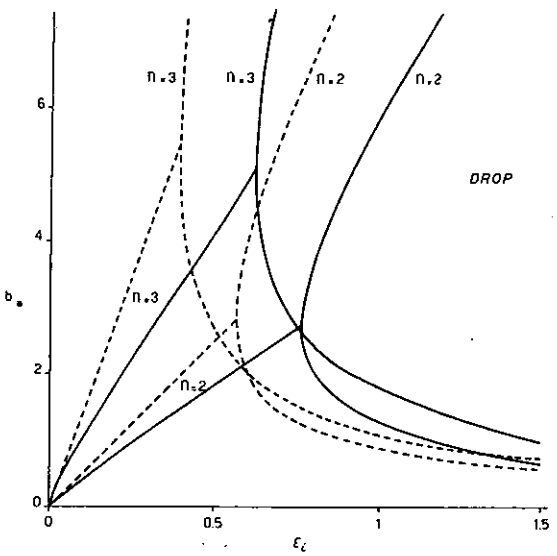

Fig. 1. – The dimensionless damping constant b_* (real part of the eigenvalue σ_*) as a function of the dimensionless viscosity ε_i, equation (44), for the oscillations of a viscous liquid drop in a medium of negligible dynamical effects (e. g., air) for the modes $n=2$ and $n=3$. The dashed curves correspond to the solutions of equation (42), which is valid for small viscosity. For each curve a critical value of the viscosity exists above which the eigenvalues σ_* become purely real. This behavior is indicated by the branching of the curves. The upper branch is in effect the second eigenvalue.

bubble. Letting $\mu_i \to 0$, $\rho_i \to 0$ and making use of (41) we readily obtain from (32):

$$T_0(R) = -\frac{\mathscr{H}^{(1)}_{n-(1/2)}(X_0)}{1+(1/2)\mathscr{H}^{(1)}_{n-(1/2)}} \frac{n+2}{n+1}\sigma a.$$

The characteristic equation (33) reduces now to:

$$(45) \qquad (\sigma^2 - 2b_B\sigma + \omega_B^2)[\mathscr{H}^{(1)}_{n-(1/2)}(X_0)+2] + 4n(n+2)^2\frac{\nu_0}{R^2}\sigma = 0,$$

where:

$$(46) \qquad \begin{cases} \omega_B^2 = (n-1)(n+1)(n+2)\zeta/\rho_0 R^3, \\ b_B = (n+2)(2n+1)\nu_0/R^2, \end{cases}$$

again are the frequency and damping constant for small viscosity ([8], p. 475 and p. 639).

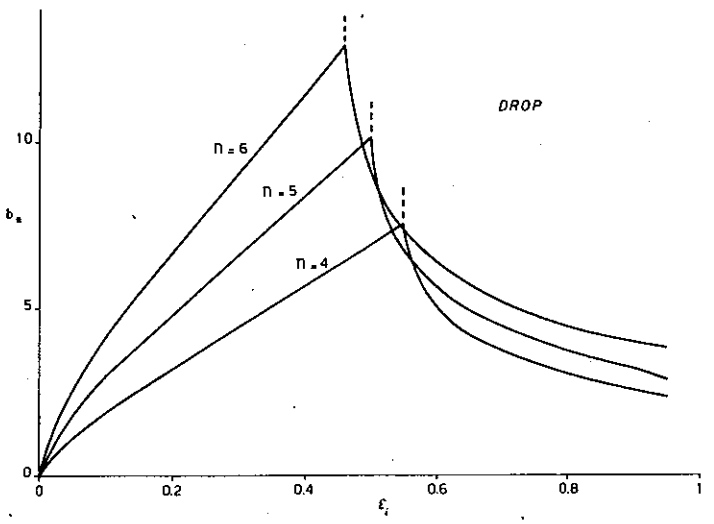

Fig. 2. – The dimensionless damping constant b_* (real part of the eigenvalue σ_*) as a function of the dimensionless viscosity ε_i, equation (44), for the oscillations of a viscous liquid drop in a medium of negligible dynamical effects (e. g., air) for the modes $n=4$, $n=5$, and $n=6$. For each curve a critical value of the viscosity exists above which the eigenvalues σ_* become purely real. This behavior is indicated by the branching of the curves.

It is readily seen that the function $\mathscr{H}^{(1)}_{n-(1/2)}$ reduces to the quotient of two polynomials. The characteristic equation (45) therefore has only a finite number of roots, and completeness of eigenvalues and eigenvectors can only be achieved including the continuous spectrum.

Since the function $\mathscr{H}^{(1)}_{n-(1/2)}$ is complex when its argument is real equation (45) cannot have real roots. As a consequence, in contrast with the drop case, it is seen that the oscillations cannot be exactly overdamped no matter how large the viscosity. This feature is caused by the convexity of the free surface and by the infinite extent of the fluid which allow a very efficient smoothing process of the velocity gradients. A purely real value of σ is obtained only as an approximation for large viscosity since:

$$\mathscr{H}^{(1)}_{n-(1/2)}(X) \simeq 2n-1-\frac{1}{2n-3}X^2, \quad \text{for} \quad X \to 0, \tag{47}$$

so that the least damped root of (45) becomes:

$$\sigma \simeq \frac{2n+1}{2(n+2)(2n^2+1)} \frac{R^2 \omega_B^2}{\nu_0}.$$

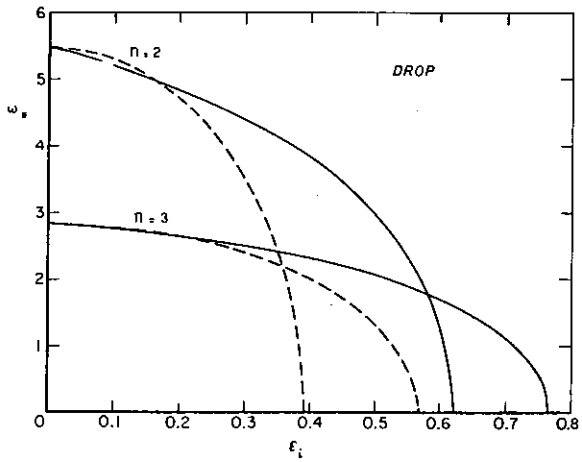

Fig. 3. – The dimensionless frequency ω_* (imaginary part of the eigenvalue σ_*) as a function of the dimensionless viscosity ε_i, equation (44), for the oscillations of a viscous liquid drop in a medium of negligible dynamic effects (e. g., air) for the modes $n=2$ and $n=3$. The dashed curves correspond to the solutions of equation (42), which is valid for small viscosity. For each curve a critical value of the viscosity exists above which the eigenvalues σ_* become purely real. The approximate equation (42) underestimates substantially the location of this point.

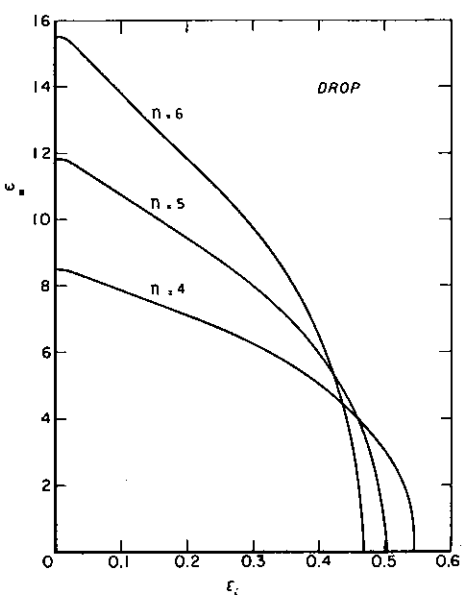

Fig. 4. – The dimensionless frequency ω_* (imaginary part of the eigenvalue σ_*) as a function of the dimensionless viscosity ε_i, equation (44), for the oscillations of a viscous liquid drop in a medium of negligible dynamical effects (e. g., air) for the modes $n=4$, $n=5$, $n=6$. For each curve a critical value of the viscosity exists above which the eigenvalues σ_* become purely real.

Also in this case the complex roots occur in pairs since:

$$\overline{\mathscr{H}^{(1)}_{n-(1/2)}(X)} = \mathscr{H}^{(2)}_{n-(1/2)}(\bar{X}),$$

and $\mathscr{H}^{(2)}_{n-(1/2)}$ should be chosen in (27) when $\mathrm{Im}\,\sigma<0$.

We have solved equation (45) numerically for the least damped normal mode in terms of the nondimensional quantities:

$$\sigma_* = (\rho_0 R^3/\zeta)^{1/2}\sigma, \qquad \varepsilon_0 = \nu_0(\rho_0/R\,\zeta)^{1/2}, \tag{48}$$

which are analogous to those previously used in the drop case. Figures 5 and 6 show:

$$b_* = \mathrm{Re}\,\sigma_*, \qquad \omega_* = \mathrm{Im}\,\sigma_*,$$

respectively for $n=2, 3$, whereas Figures 7 and 8 refer to $n=4, 5, 6$. For the two smaller values of n also the solutions of the approximate equation:

$$\sigma^2 - 2b_B\sigma + \omega_B^2 = 0, \tag{49}$$

which, like (42), is valid for small viscosity, are shown. Notice that the roots of this equation exhibit a changeover from oscillatory to aperiodic motion when ε_0 increases beyond a critical value. Althoug the root of (45) is seen to agree with that of (49) for small ε_0, the deviation between the two is much stronger for a fixed value of ε_0 for the bubble than for the drop case. This behavior is physically understandable because the effect of vorticity diffusion in the unbounded domain and "de-focussing" geometry of the bubble case is necessarily greater than that in the bounded domain and "focussing" geometry of the drop. It is more difficult to compare on absolute terms the rates of damping for fixed ε_0 for the bubble and drop cases. Such a comparison should be made in an initial-value-problem context, and there it would be found that the continuous spectrum in general gives rise to an algebraic, rather than exponential, decay in time of the motion for the bubble [4].

An interesting feature exhibited by $b_* = \mathrm{Re}\,\sigma_*$ in Figures 5 and 7 is the maximum of each curve, which can be compared with the much sharper one taking place in the drop case (*Figs.* 1 and 3) in correspondence with the change-over to aperiodic motion. This structure of the dependence of the damping constant on viscosity is related to the presence in this problem of two different length scales, the radius R and the diffusion length for momentum, or vorticity, which is of order $(\nu_0/\omega_B)^{1/2}$. The structure of the vorticity distribution is different if $R>(\nu_0/\omega_B)^{1/2}$ (i. e. ε_0 small) or $R<(\nu_0/\omega_B)^{1/2}$

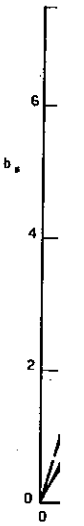

Fig. 5. – Th
function of
gas bubble
a behavior
equation (4
transition t

Fig. 6. – The
function of
permanent g
which exhibi
the solutions
solution no

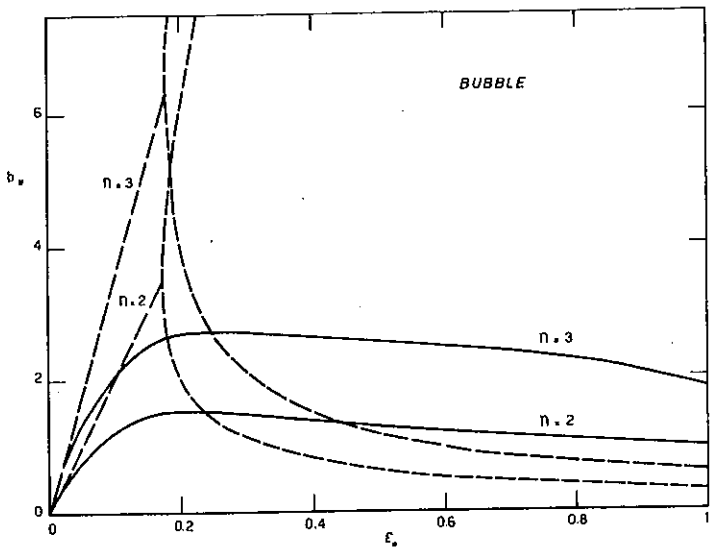

Fig. 5. – The dimensionless damping constant b_* (real part of the first eigenvalue σ_*) as a function of the dimensionless viscosity ε_0, equation (48), for the shape oscillations of a permant gas bubble in a viscous liquid for the modes $n=2$ and $n=3$. The dashed curves, which exhibit a behavior similar to the onefound in the drop case of Figure 1, correspond to the solutions of equation (49), which is valid for small viscosity. Notice that for the exact solution no transition to aperiodic motion exists.

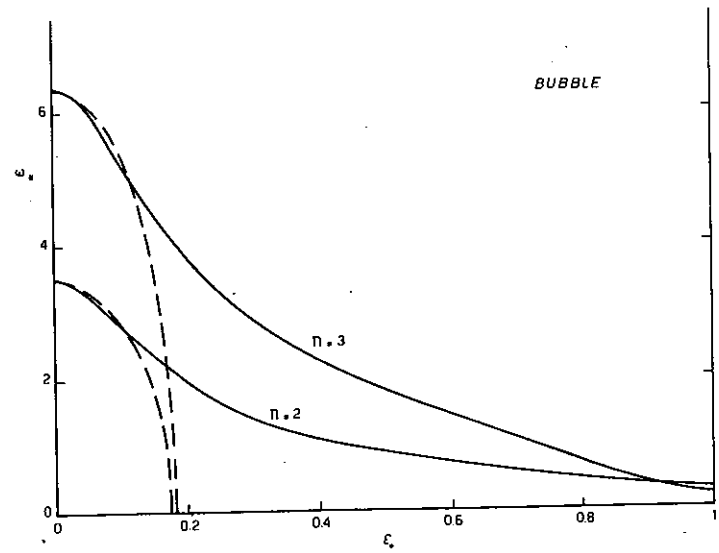

Fig. 6. – The dimensionless frequency ω_* (imaginary part of the first eigenvalue σ_*) as a function of the dimensionless viscosity ε_0, equation (48), for the shape oscillations of a permanent gas bubble in a viscous liquid for the modes $n=2$ and $n=3$. The dashed curves, which exhibit a behavior similar to the one found in the drop case of Figure 3, correspond to the solutions of equation (49), which is valid for small viscosity. Notice that for the exact solution no transition to aperiodic motion exists.

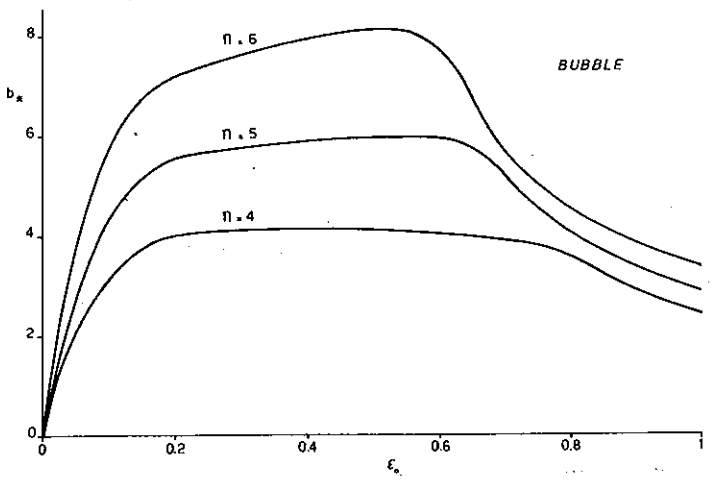

Fig. 7. — The dimensionless damping constant b_* (real part of the first eigenvalue σ_*) as a function of the dimensionless viscosity ε_0, equation (48), for the shape oscillations of a permanent gas bubble in a viscous liquid for the modes $n=4$, $n=5$, and $n=6$. Notice that, in contrast with the drop case of Figure 2, transition to aperiodic motion does not occur.

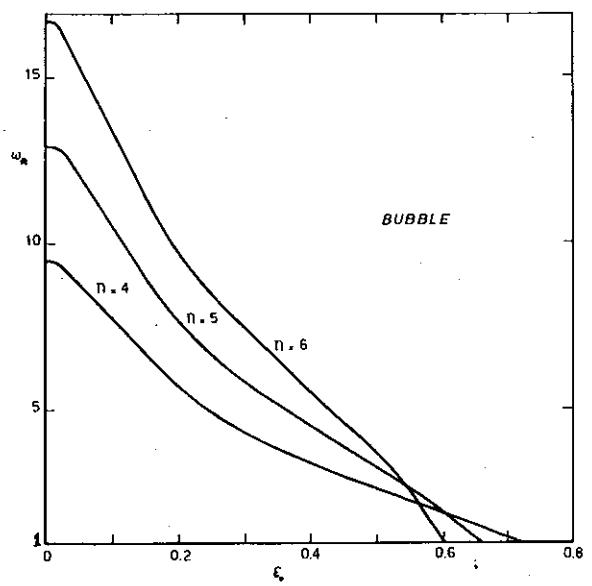

Fig. 8. — The dimensionless frequency ω_* (imaginary part of the first eigenvalue σ_*) as a function of the dimensionless viscosity ε_0, equation (48), for the shape oscillations of a permanent gas bubble in a viscous liquid for the modes $n=4$, $n=5$, and $n=6$. For large viscosity the curves tend to zero only asymptotically.

(i. e. ε_0 large). In the second case the motion is so effectively inhibited that $\mathrm{Re}\,\sigma_*$, which measures essentially the energy dissipation per unit time, starts to decrease with increasing viscosity.

For small ε_0 one deduces from (45) the following approximate form for the relationship $\sigma_* = \sigma_*(\varepsilon_0)$:

$$\sigma_* \simeq i\omega_{B_*} + (n+2)(2n+1)\varepsilon_0 \pm \varepsilon_0^{3/2}(1+i)\,2^{1/2}\,n(n+2)^2\,\omega_{B_*}^{-1/2} + \ldots$$

The double sign shows the coalescence of the first two normal modes into the solution of (49) as $\varepsilon_0 \to 0$.

The results for a plane surface can be recovered from (45) if one observes that $k = n/R$ is the wave number of the surface waves of the n-th mode. Therefore, to obtain the characteristic equation for waves of wavelength $2\pi/k$ over a plane surface we let $R \to \infty$, $n \to \infty$ with k fixed. Making use of the asymptotic formulas for Bessel functions of large order and large variable [25] it is a simple matter to show that:

$$\mathscr{H}^{(1)}_{n-(1/2)}(R(\sigma/\nu)^{1/2}) \sim n\left[\left(1-\frac{\sigma}{\nu k^2}\right)^{1/2}+1\right].$$

Substitution into (45) results in the well-known characteristic equation for capillary waves over a plane surface ([8], p. 627; [24]):

$$(\sigma - 2\nu k^2)^2 + k^3\,\zeta/\rho - 4(\nu k^2)^{3/2}(\nu k^2 - \sigma)^{1/2} = 0.$$

In conclusion we consider briefly the continuous spectrum. The form of equations (36 *b*) and (37) appropriate to the present case is:

$$(50)\quad 2(n+1)X_0^{-1/2}(M_0 J_{n-(1/2)} + N_0 Y_{n-(1/2)}) + (n+1)X_0^{1/2}(M_0 J_{n+(1/2)} + N_0 Y_{n+(1/2)}) = -2(n+2)\sigma a,$$

$$(51)\quad n(n+1)(n+2)\frac{\nu_0 X_0^{1/2}}{R}(M_0 J_{n+(1/2)} + N_0 Y_{n+(1/2)}) = -\left[\sigma^2 + 2(n-1)(n+1)(n+2)\frac{\nu_0}{R^2}\sigma + \omega_B^2\right] a.$$

Solving for M_0, N_0 we find:

$$(52)\quad M_0 = \frac{1}{4}\pi\left\{2\frac{n+2}{n+1}\sigma X_0 Y_{n+(1/2)} + \frac{R^2}{n(n+1)(n+2)\nu_0}(2Y_{n-(1/2)} + X_0 Y_{n+(1/2)}) \times \left[\sigma^2 + 2(n-1)(n+1)(n+2)\frac{\nu_0}{R^2}\sigma + \omega_B^2\right]\right\} X_0^{1/2}\, a,$$

$$(53)\quad N_0=\frac{1}{4}\pi\left\{\frac{R^2}{n(n+1)(n+2)\nu_0}(2J_{n-(1/2)}+X_0J_{n+(1/2)})\times\left[\sigma^2+2(n-1)(n+1)(n+2)\frac{\nu_0}{R^2}\sigma+\omega_B^2\right]-2\frac{n+2}{n+1}X_0J_{n+(1/2)}\sigma\right\}X_0^{1/2}a.$$

It is interesting to show the limiting form of $T_0(R)$ for $\sigma\to 0$. From the above results and (27 *b*) one finds:

$$T_0(R)\simeq-\frac{1}{n(n+1)(n+2)}\frac{\omega_B^2R^2}{\nu_0}a,$$

which is different from zero thus exhibiting explicitly the eigenvalue nature of $\sigma=0$ in agreement with the general theory [23].

7. Drop in an immiscible liquid

We shall consider now the complete characteristic equation (33). On the basis of the asymptotic expressions (38) and (41) it is possible to obtain the following approximate expression for σ:

$$(54)\quad \sigma\simeq\frac{(2n+1)^2(\omega\mu_i\mu_0\rho_i\rho_0)^{1/2}}{\sqrt{2}\gamma}-\frac{(2n+1)^4\rho_i\rho_0\mu_i\mu_0}{\gamma^2}+\frac{\left\{\begin{array}{l}(2n+1)\{2(n-1)(n+1)\mu_i^2\rho_i+2n(n+2)\mu_0^2\rho_0\\ \qquad+\mu_0\mu_i[(n+2)\rho_i-(n-1)\rho_0]\}\end{array}\right\}}{R\gamma[(\mu_i\rho_i)^{1/2}+(\mu_0\rho_0)^{1/2}]}\pm i\left[\omega-\frac{(2n+1)^2(\omega\mu_i\mu_0\rho_i\rho_0)^{1/2}}{\sqrt{2}\gamma}\right],$$

where ω is given by (34) and:

$$\gamma=2R[n\rho_0+(n+1)\rho_i][(\mu_i\rho_i)^{1/2}+(\mu_0\rho_0)^{1/2}].$$

The result (54) is obtained on the assumption that ν_i and ν_0 are both small and of the same order of magnitude. By comparing it with the numerical solution of the characteristic equation it is found that it predicts values within about 10 % of the exact ones provided that $\nu(\rho/R\zeta)^{1/2}\lesssim 0.1$. The accuracy however gets worst if the values of this dimensionless group for the two

fluids, though remaining small, are made of different order of magnitude. Equation (54) was first given by Miller and Scriven [13] who however apparently overlooked the second term in the real part.

For $\mu_i=\mu_0=0$ equation (54) reduces to $\sigma=\pm i\omega$ thus justifying the statement on the physical meaning of ω made after equation (34). The approximate expression for large viscosity can be obtained with the aid of (43) and (47) in the form [13]:

$$\sigma=\frac{(2n+1)(\mu_0+\mu_i)R^2[n\rho_0+(n+1)\rho_i]\omega^2}{\left\{\begin{array}{r}2\mu_i^2(n^2-1)(2n^2+4n+3)+2\mu_0^2 n(n+2)(2n^2+1)\\ +\mu_0\mu_i[8n(n^2-1)(n+2)+3(2n+1)^2]\end{array}\right\}}.$$

In order to present some numerical results relative to the complete equation (33) let us set:

$$\sigma_*=(\rho_i R^3/\zeta)^{1/2}\sigma, \tag{55}$$

$$\varepsilon_i=\nu_i(\rho_i/R\zeta)^{1/2}, \qquad \varepsilon_0=\nu_0(\rho_0/R\zeta)^{1/2},$$

$$\mu=\mu_0/\mu_i, \qquad \rho=\rho_0/\rho_i.$$

The characteristic equation becomes then:

$$\begin{aligned}(n\rho+n+1)&[\mathscr{I}_{n+(3/2)}(X_i)+\mu\,\mathscr{K}^{(1)}_{n-(1/2)}(X_0)+2(\mu-1)](\sigma_*^2+\omega_*^2)\\ &-\sigma_*[(2n+1)\mathscr{I}_{n+(3/2)}(X_i)+2n(n+2)(\mu-1)]\\ &\times[(2n+1)\mu\,\mathscr{K}^{(1)}_{n-(1/2)}(X_0)-2(n-1)(n+1)(\mu-1)]=0,\end{aligned} \tag{56}$$

where:

$$X_i=(\sigma_*/\varepsilon_i)^{1/2}, \qquad X_0=(\sigma_*/\varepsilon_0)^{1/2},$$

$$\omega_*=\frac{(n-1)n(n+1)(n+2)}{n\rho+n+1}.$$

It is seen that the eigenvalue σ_* depends now on three dimensionless parameters which may be chosen as $\rho, \varepsilon_i, \varepsilon_0$. Some examples of the results obtained in this case are shown in Figures 9 to 16 for $n=2$.

Figure 9 shows the dimensionless damping constant $b_*=\mathrm{Re}\,\sigma_*$ when the outer fluid is much lighter than the inner one, $\rho_0/\rho_i=0.1$. The results for $\rho_0=0$, $\varepsilon_0=0$ of Figure 1 are also included in this figure for comparison (dotted line). The curves exhibit a pronounced maximum, analogous to the one which appeared in the bubble case, which has the same physical origin

and which marks the passage to the "creeping motion" regime. It is seen that for small or moderate values of the viscosity of the outer fluid ($\varepsilon_0 \lesssim 0.2$) there is comparatively little influence of the presence of the outer fluid since the curves are relatively close to one another. The situation is different when the viscosity of the outer fluid becomes large, its density remaining one tenth

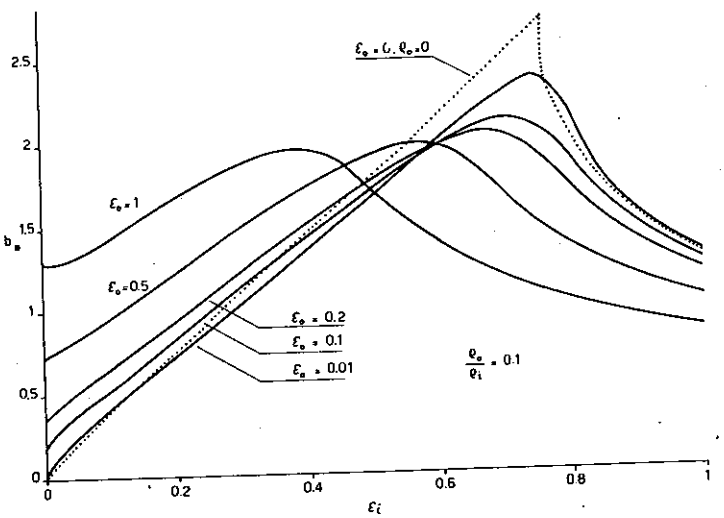

Fig. 9. — The dimensionless damping constant b_* (real part of the first eigenvalue σ_*) as a function of the dimensionless viscosities of the inner, ε_i, and outer, ε_0, equation (55), fluids for the oscillations of a viscous liquid drop in a viscous immiscible liquid for $n=2$. The inner fluid is a factor of ten denser than the outer one. The dashed curve is the same as the drop-in-air case shown by the solid curve in Figure 1.

that of the inner fluid. Figure 10 shows similar results when the outer fluid is much denser than the inner one, $\rho_0/\rho_i = 10$. The rate of damping drops by an order of magnitude in comparison with the previous case since the motion [measured on the time scale of the inner fluid, *see* equation (55)] slows down considerably. It is also seen that, except for the case $\varepsilon_0 = 0.01$, the influence of the viscosity of the inner fluid is very small. This circumstance can be understood recalling that, from the definitions (55), we have $\mu_i/\mu_0 = (\varepsilon_i/\varepsilon_0)(\rho_i/\rho_0)^{1/2}$. Hence, for ε_i and ε_0 of the same order, the dynamic viscosity of the inner fluid relative to that of the outer one decreases with increasing ρ_0/ρ_i and hence, for large values of this ratio, the effect of the inner fluid on the motion of the outer one becomes small. A peculiar feature of the curves for $\varepsilon_0 = 0.1$ and 0.2, which can also be noticed in those of Figure 11 for $\rho_0 = \rho_i$, is the shallow minimum which appears as ε_i increases

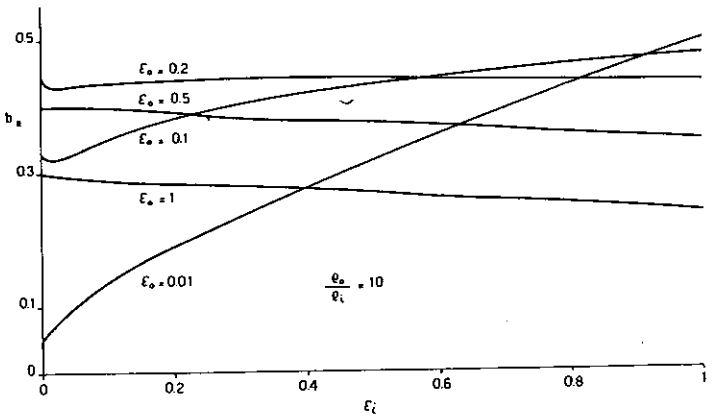

Fig. 10. – Same as Figure 9
when the outer fluid is a factor of 10 denser than the inner one.

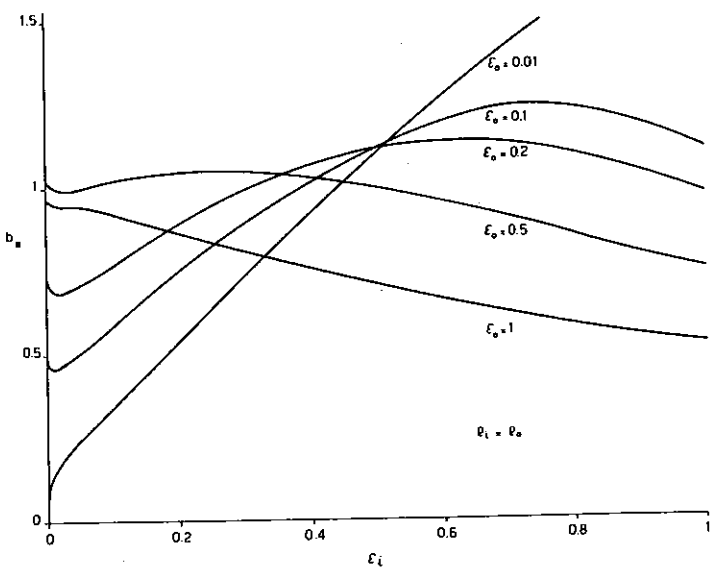

Fig. 11. – Same as Figure 9
when inner and outer fluids have equal densities.

away from zero. This behavior shows the profound effect that the second fluid has on the boundary layer structure of the system because of the no-slip condition. As soon as ε_i is greater than zero the continuity of velocities entails a substantial decrease of the stresses, and hence of the rate of damping (*see* e. g. [26]).

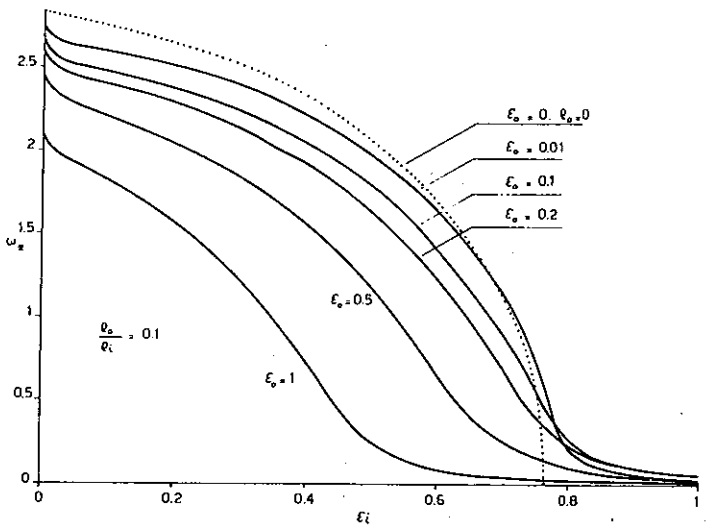

Fig. 12. – The dimensionless frequency ω_* (imaginary part of the lowest eigenvalue σ_*) as a function of the dimensionless viscosities of the inner, ε_i, and outer, ε_0, equation (55), fluids for the oscillations of a viscous liquid drop in a viscous immiscible liquid for $n=2$. The inner fluid is a factor of ten denser than the outer one. The dashed curve is the same as the drop-in-air case shown by the solid curve in Figure 3.

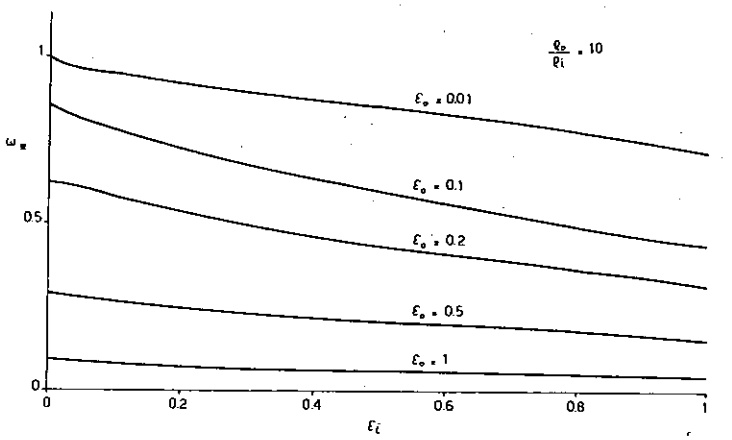

Fig. 13. – Same as Figure 12
when the outer fluid is a factor of 10 denser than the inner one.

In Figure 12 the frequency of oscillation $\omega_* = \mathrm{Im}\,\sigma_*$ is shown for $\rho_0/\rho_i = 0.1$; the results for a drop in vacuum (i.e. $\rho_0 = 0$, $\varepsilon_0 = 0$) are also shown as a dotted line for comparison. It is seen that, as in the bubble case, $\mathrm{Im}\,\sigma_*$ is never zero although it does approach this value for large

viscosities. Again, as in the case of b_*, significant differences appear only for relatively large values of ε_0. The abrupt drop as ε_i grows away from zero (which is also evident in Figure 14 for $\rho_i = \rho_0$) is also of interest in view of the considerations made above on the consequences of the no-slip

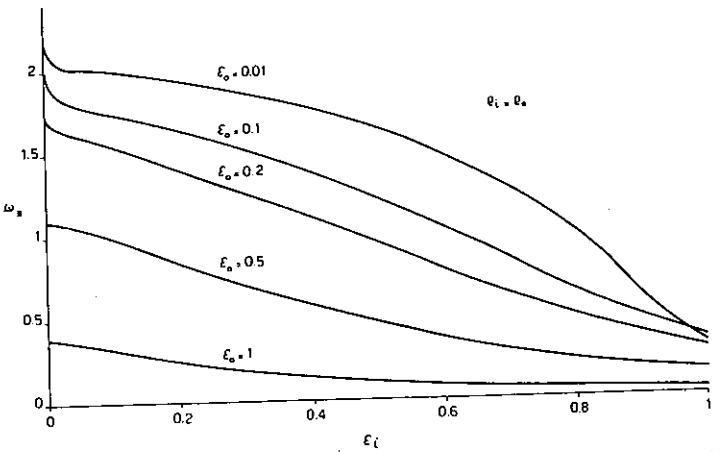

Fig. 14. — Same as Figure 12 when inner and outer fluids have equal densities.

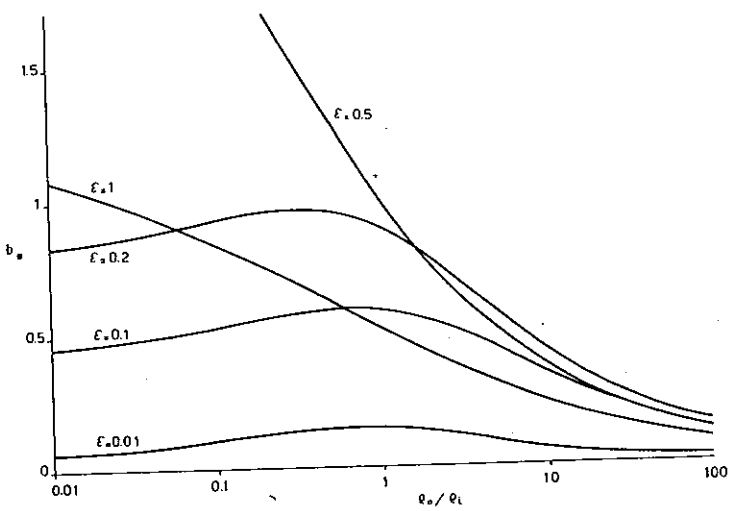

Fig. 15. — The dimensionless damping constant b_* (real part of the first eigenvalue σ_*) as a function of the ratio of the density of the outer fluid, ρ_0, to that of the inner one, ρ_i, for the oscillations of a viscous liquid drop in a viscous immiscible liquid for $n=2$. The different curves correspond to different values of the dimensionless viscosities (55), which are taken to be equal, $\varepsilon_0 = \varepsilon_i = \varepsilon$.

condition. Comparing with Figure 9 it is seen that the rapid change in concavity takes place in the interval in which b_* has its maximum, just as in the bubble case. The corresponding results for $\rho_0/\rho_i = 10$ are shown in Figure 13. As was noticed before, the large inertia causes a substantial slowing down of the oscillations, which appear to be much more sensitive to the viscosity of the outer fluid than to that of the inner one. Many of the characteristics found in the cases $\rho_i/\rho_0 = 0.1$ and $\rho_i/\rho_0 = 10$ are combined in

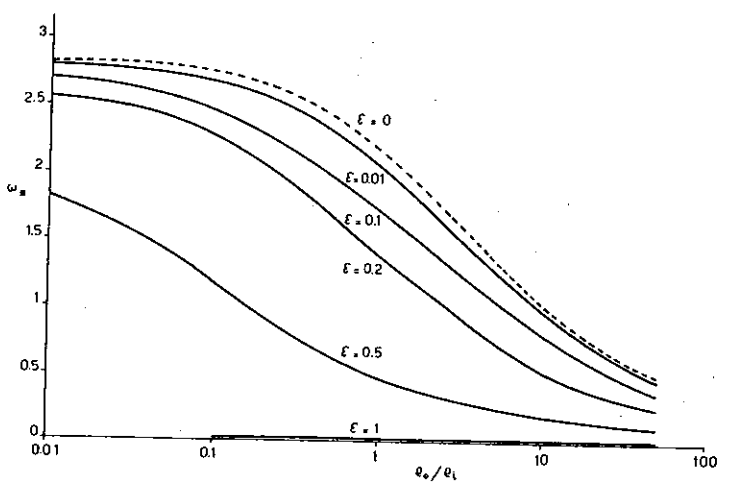

Fig. 16. – The dimensionless frequency ω_* (imaginary part of the first eigenvalue) as a function of the ratio of the density of the outer fluid, ρ_0, to that of the inner one, ρ_i, for the oscillations of a viscous liquid drop in a viscous immiscible liquid for $n=2$. The different curves correspond to different values of the dimensionless viscosities (55), which are taken to be equal, $\varepsilon_0 = \varepsilon_i = \varepsilon$. The dashed curve, labelled by $\varepsilon = 0$, is the frequency for the inviscid case given by equation (34).

the intermediate one $\rho_i = \rho_0$ to which Figures 11 and 14 refer. This case is particularly interesting from a pratical viewpoint because the density differences of immiscible liquids in emulsions are usually small. Furthermore, our neglect of external force fields such as gravity becomes exactly valid in this case.

An illustration of the dependence of the results on ρ_0/ρ_i is given in Figures 15 and 16 which show b_* and ω_* as a function of this ratio for several values of $\varepsilon_i = \varepsilon_0 = \varepsilon$. In Figure 16 the dashed line corresponds to the inviscid frequency (34). An interesting feature that can be observed in Figure 15 is the non-monotonic behavior of b_* for the three smallest values of ε.

8. Comparison with experimental results

We compare now the theoretical results obtained from equation (33) with some experimental data. The Table lists the data and the calculated results, together with some relevant parameters, for the six cases reported in reference [12] relative to oscillations of drops of a carbon tetrachloride-benzene solution in water. The density of both fluids was $1\,g/cm^3$. The

TABLE

Comparison of the theoretical results computed from equation (33) *with the data of reference* [12] *and the theoretical results of reference* [13]

Drop	A	B	C	D	E	F
Radius (cm).	0.49	0.39	0.39	0.565	0.565	0.565
Initial amplitude (cm). . .	0.65	0.55	0.55	0.95	0.7	0.6
Calculated frequency $\omega/2\pi$ (sec^{-1}).	4.31	6.52	5.52	3.93	3.85	3.85
Initial oscillation frequency, $\omega/2\pi$ (sec^{-1}). . . .	4.0	7.0	5.0	4.0	5.0	5.0
Final oscillation frequency, $\omega/2\pi$ (sec^{-1}). . . .	6.0	10.0	9.0	7.5	7.0	6.0
Calculated decay time b^{-1} (sec.).	0.61	0.38	0.39	0.80	0.79	0.79
Observed decay time b^{-1} (sec.).	0.7	0.2	0.6	0.4	0.4	0.3
Decay time from reference [13] b^{-1} (sec.)..	2.3	1.5	1.5	3.1	3.1	3.1
ε_i.	0.036	0.038	0.044	0.030	0.031	0.031
$\varepsilon_0 \times 10^3$.	3.24	3.42	3.96	2.70	2.79	2.79

kinematic viscosity of the drop is not given explicitly but on the basis of some calculations reported in [12] it has been estimated to be $\nu_i = 0.111\ cm^2/sec$. The oscillations were excited by a localized change of the interfacial tension of the drop.

For what concerns the oscillation frequency one can observe a good agreement between the data relative to the initial oscillations and our theoretical results. The agreement is much less satisfactory for the data relative to the final oscillation frequency. This situation is paradoxical because, if the difference between the two sets of data were caused by nonlinear effects, as might be expected, one should have agreement of the

calculations with the data for the final oscillations. However, at a closer inspection, it appears unlikely that the large discrepancy between the initial and final data is to be imputed entirely to nonlinear effects. Indeed, in nonlinear oscillations, the frequency decreases usually as the square of the amplitude, which might be expected to introduce a difference of 10-20% between initial and final values of the oscillation frequency. For an alternative explanation we can turn to the observations of Yao and Schrock [33] who measured the oscillation frequency of drops in free fall in air. They observed that as the distance of fall increased, the oscillation frequency tended to decrease until the drop nearly stabilized about a distorded spherical shape. Although the translational velocity in the experiments of reference [12] was rather small, of the order of 2 cm/sec, it appears possible that it had a nonnegligible effect on the final stages of the oscillations, when the amplitude was greatly reduced.

Turning now to the comparison of observed and calculated decay times we find a good agreement in case A, a still acceptable one in case C, whereas the theoretical results appear to underestimate the decay times by a factor of 2 in the remaining cases. These large discrepancies may perhaps be imputed to impurities in the liquids which caused surface contamination. This event would affect the energy dissipation rate in two ways, through its efect on the translational motion, and through its modification of the rheological properties of the interface. This possibility is suggested by the well-documented difficulty in experimental work on drops and bubbles connected with the necessity of using highly purified fluids [34]. From a reading of reference [12] it does not appear that any special care was exerted to insure the purity of the liquids used.

Finally, in the Table we also give the results calculated by Miller and Scriven [13] with their (incorrect) equivalent of our equation (54). Notice the order-of-magnitude difference between the decay times reported by these authors and our results. In this connection it should be observed that, even using the correct form of the approximation for small ν, equation (54), one obtains results affected by an unacceptable error for the cases of Table.

9. Purely rotational waves

The problem relative to the S component of the vorticity embodied in equations (10), (18), (20) can be solved in a way similar to that employed above for the oscillatory modes. Let us first suppose that eigenvalues exist such

that Im $\sigma > 0$. Then the conditions of boundedness at infinity and at the center of the drop force us to write the solution of equation (10) in a form similar to equation (28), namely:

$$S_i = \left(\frac{r}{R}\right)^{1/2} S_i(R) \frac{J_{n+(1/2)}(x_i)}{J_{n+(1/2)}(X_i)},$$

$$S_0 = \left(\frac{r}{R}\right)^{1/2} S_0(R) \frac{H^{(1)}_{n+(1/2)}(x_0)}{H^{(1)}_{n+(1/2)}(X_0)}.$$

The two boundary conditions determine $S_i(R)$, $S_0(R)$ up to a multiplicative factor and give rise to the following characteristic equation:

$$\mu_0 \mathscr{H}^{(1)}_{n+(1/2)}(X_0) - \mu_i \mathscr{J}_{n+(1/2)}(X_i) = (\mu_0 - \mu_i)(n+2),$$

where:

$$\mathscr{H}^{(1)}_{\nu}(z) = z H^{(1)}_{\nu-1}(z)/H^{(1)}_{\nu}(z).$$

Miller and Scriven [13] quote a result of Bupara according to which the only roots of this characteristic equation are purely real. This circumstance is exactly as expected, because the modes under consideration do not generate a restoring force capacle of giving rise to an oscillatory behavior. Thus, the assumption Im $\sigma > 0$ under which the characteristic equation was derived is not satisfied. Therefore, for the outer field we are allowed to write the solution for S in the same form (27 *b*) used in the analysis of the continuous spectrum for the shape oscillations. The considerations made above in Section 4 then apply to the rotational "wave" motion as well and, in contrast with [13], we are led to the conclusion that the spectrum for these modes is purely continuous and consists of the entire non-negative real semi-axis.

10. Note on the numerical method

Use of the quotients of Bessel functions is especially convenient for numerical computation because it is easily verified that the functions $\mathscr{J}_{\nu}(z)$ and $\mathscr{H}^{(1)}_{\nu}(z)$ satisfy the relationships [18] :

$$\mathscr{J}_{\nu}(z) = \frac{z^2}{2(\nu-1) - \mathscr{J}_{\nu-1}(z)},$$

$$\mathscr{H}^{(1)}_{\nu}(z) = 2\nu - z^2/\mathscr{H}^{(1)}_{\nu-1}(z).$$

Since:

$$\mathscr{J}_{1/2}(z)=z\cot z,$$
$$\mathscr{H}^{(1)}_{1/2}(z)=1-iz,$$

these recursive relations can be used to compute the value of the function for any index of the form $n+(1/2)$.

An efficient algorithm for the computation of the roots of the characteristic equations was found to be the (tangent) Newton-Raphson method. For each value of n the values of σ_* were computed in succession for increasing ε. For the two one-liquid cases and the smallest value of ε (typically in the range 0.01-0.1) use was made of the expressions for σ_* obtained from (42) and (49) as initial guesses in the iterative process. The initial guess for the subsequent values of ε was taken as the value of σ_* found for the preceding value. In this way convergence to within 1 part in 10^5 was obtained in usually 3-5 interactions for increments in ε of up to 0.2.

A similar procedure was used for the two-liquid computations. Here however no analytic expression was available for use as initial guess. Therefore the limiting value of (33) for $\varepsilon_i \to 0$ was considered, namely:

$$(57)\quad \left[1+\frac{1}{2}\mathscr{H}^{(1)}\right]\left[\sigma_*^2+\omega_*^2+2\frac{n(n+2)(2n+1)}{n+(n+1)\rho_i/\rho_0}\varepsilon_0\sigma_*\right] -2\frac{n^2(n+2)^2}{n+(n+1)\rho_i/\rho_0}\varepsilon_0\sigma_*=0.$$

The roots of this equation were computed as described above for increasing values of ε_0, using as initial guess for small ε_0 the following expression which generalizes (49) to the case $\rho_i>0$ and which is readily obtained from (57):

$$\sigma_*\simeq i\omega_*+\frac{n(n+2)(2n+1)}{n+(n+1)\rho_i/\rho_0}\varepsilon_0.$$

The roots of (57) were then used as starting points to compute the roots of the complete equation (33) for increasing values of ε_i as described above.

It was found that in the bubble and in the two-fluid cases the second normal mode could easily be generated by the above procedure using $\mathscr{H}^{(2)}_{n-(1/2)}$ in place of $\mathscr{H}^{(1)}_{n-(1/2)}$. In this way however, since the two functions are one the complex conjugate of the other, Im σ_* turned out to be negative. No simple way was found for the computation of the second root of the drop-in-vacuum

case, which was obtained in a few cases by trial and error. In general it was found that both b_* and ω_* increase rapidly with viscosity for these second modes, which justifies their neglect in the present study.

REFERENCES

[1] BATCHELOR G. K., *Transport Properties of Two-Phase Materials with Random Structure* (*Ann. Rev. Fluid Mech.*, Vol. 6, 1974, pp. 227-255).

[2] HARPER J. F., *The Motion of Bubbles and Drops Through Liquids* (*Adv. Appl. Mech.*, Vol. 12, 1972, pp. 59-129).

[3] SUBRAMANYAM S. V., *A Note on the Damping and Oscillations of a Fluid Drop Moving in Another Fluid* (*J. Fluid Mech.*, Vol. 37, 1969, pp. 715-725).

[4] PROSPERETTI A., *Shape Oscillations of Drops and Bubbles: the Initial-Value Problem* (*J. Fluid. Mech.*, in press).

[5] *Proceedings of the International Colloquium on Drops and Bubbles*, COLLINS D. J., PLESSET M. S. and SAFFREN M. M. Ed., Jet Propulsion Laboratory, Pasadena, 1976.

[6] Lord KELVIN, *Oscillations of a Liquid Sphere*, in *Mathematical and Physical Papers*, Clay and Sons, London, 1890, Vol. 3, pp. 384-386.

[7] Lord RAYLEIGH, *The Theory of Sound*, 2nd Ed., MacMillan, London, 1894 (reprinted by Dover, New York, 1945), Vol. 2, p. 371.

[8] LAMB H., *Hydrodynamics*, 6th Ed., Cambridge University Press, Cambridge, 1932 (reprinted by Dover, New York, 1945).

[9] CHANDRASEKHAR S., *The Oscillations of a Viscous Liquid Globe* (*Proc. London Math. Soc.*, Vol. 9, 1959, pp. 141-149).

[10] CHANDRASEKHAR S., *Hydrodynamic and Hydromagnetic Stability*, Clarendon Press, Oxford, 1961.

[11] REID W. H., *The Oscillations of a Viscous Liquid Drop* (*Quart. Appl. Math.*, Vol. 18, 1960, pp. 86-89).

[12] VALENTINE R. S., SATHER N. F. and HEIDEGER W. J., *The Motion of Drops in Viscous media* (*Chem. Eng. Sc.*, Vol. 20, 1965, pp. 719-728).

[13] MILLER C. A. and SCRIVEN L. E., *The Oscillations of Fluid Droplets Immersed in Another Fluid* (*J. Fluid Mech.*, Vol. 32, 1968, pp. 417-435).

[14] TONG H. H. K. and WONG C. Y., *Vibrations of a Viscous Liquid Sphere* (*J. Phys. A*, Vol. 7, 1974, pp. 1038-1050).

[15] WONG C. Y., *Limits of the Nuclear Viscosity Coefficuent in the Liquid Drop Model* (*Phys. Lett. B*, Vol. 61, 1976, pp. 321-323).

[16] MORSE P. M. and FESHBACH H., *Methods of Theoretical Physics*, McGraw-Hill, New York, 1953, Chap. 13.

[17] GIBBS J. W., *Scientific Papers*, Longmans, Green and Co., New York, 1906 (reprinted by Dover, New York, 1961), Vol. 1, pp. 219-231.

[18] ONOE M., *Tables of Modified Quotients of Bessel Functions*, Columbia University Press, New York, 1958.

[19] ERDÉLYI A., MAGNUS W., OBERHETTINGER F. and TRICOMI F. G., *Higher Transcendental Functions*, McGraw-Hill, New York, 1953, Vol. 2, Chap. 7.

[20] COURANT R. and HILBERT D., *Methods of Mathematical Physics*, Interscience, New York, 1953, Vol. 1, p. 339.

[21] MESSIAH A., *Quantum Mechanics*, North Holland, Amsterdam, 1965, or *Mécanique quantique*, Dunod, Paris, 1959, Chap. 5.

[22] LANDAU L. and LIFSHITZ E., *Mécanique quantique*, Mir, Moscow, 1966, or *Quantum Mechanics*, Pergamon Press, London, 1958, § 5, 21.

[23] LADYZHENSKAYA O. A., *The Mathematical Theory of Viscous Incompressible Flow*, Gordon and Breach, New York, 1963, Chap. 2.

[24] PROSPERETTI A., *Viscous Effects on Small-Amplitude Surface Waves* (*Phys. Fluids*, Vol. 19, 1976, pp. 195-203).

[25] GRADSHTEYN I. S. and RYZHIK I. M., *Tables of Series, Integrals and Products*, Academic Press, New York, 1965, p. 961.

[26] BATCHELOR G. K., *An Introduction to Fluid Dynamics*, Cambridge University Press, Cambridge, 1970, p. 346.

[27] APFEL R. E., *A Novel Technique for Measuring the Strength of Liquids* (*J. Acoust. Soc. Am.*, Vol. 49, 1971, pp. 145-155).

[28] APFEL R. E., *Tensile Strength of Superheated n-Hexane Droplets* (*Nature Phys. Sc.*, Vol. 233, 1971, pp. 119-121).

[29] APFEL R. E., *Technique for Measuring the Adiabatic Compressibility, Density, and Sound Speed of Submicroliter Liquid samples* (*J. Acoust. Soc. Am.*, Vol. 59, 1976, pp. 339-343).

[30] MARSTON P. L. and APFEL R. E., *Acoustically Forced Shape Oscillations of Hydrocarbon Drops Levitated in Water* (*J. Colloid Interface Sc.*, Vol. 68, 1979, pp. 280-286).

[31] PROSPERETTI A., *Viscous Effects on Perturbed Spherical Flows* (*Quart. Appl. Math.*, Vol. 35, 1977, pp. 339-352).

[32] GROSCH C. E. and SALWEN H., *The Continuous Spectrum of the Orr-Sommerfeld Equation* (*J. Fluid Mech.*, Vol. 87, 1978, pp. 33-54).

[33] YAO S. C. and SCHROCK V. E., *Heat and Mass Transfer from Freely Falling Drops* (*J. Heat Transfer*, Vol. 98, 1976, pp. 120-126).

[34] RAMABHADRAN T. E., BYERS C. H. and FRIEDLY J. C., *On the Dynamics of Fluid Interfaces* (*A.I.Ch.E.J.*, Vol. 22, 1976, pp. 872-882).

(Manuscrit reçu le 12 octobre 1978,
révisé le 1er mars 1979)